Magnetic Resonance Image Construction

Balew Getahun Gelaw (balew@aims.ac.za)
African Institute for Mathematical Sciences (AIMS)

Supervised by Dr. Mark W. Swanepoel
iThemba Labs

June 8, 2007

Abstract

In the advancement of medical technology, magnetic resonance imaging (MRI) technique is at the forefront. MRI is based on the interaction of nuclear spins in tissue with strong external magnetic fields $\overrightarrow{B_0}$. This magnetic field causes the nuclear spins to precess with frequency $\omega_0 = \gamma B_0$, called Larmor frequency. Two basic features make MRI practical. The first feature is that the Larmor frequency of the nuclear spins in a magnetic field depends on the local magnetic field. This fact is used to localise the MRI signals from particular parts of a tissue. To do this we apply an oscillating magnetic field $\overrightarrow{B_1}$ and a spatially-varying magnetic field with a certain gradient G_r on the tissue. The second feature is that the longitudinal magnetisation recovery time T_1 (spin-lattice relaxation time) and the transversal magnetisation decay time T_2 (spin-spin relaxationtime) are very sensitive to the substance and chemical composition differences of tissues. This provides the motivation for the selection of T_1 or T_2 as the parameter to contrast the signals from tissues. In this essay these concepts are described in detail.

ጭብጥ

ለ ህክምናው ቴክኖሎጂ ምጥቀት የመግንጢሳዊ ነዛሪነት ምስል (መነም) ዘዴ ግንባር ቀደም ነው። እሱም መሰረት የሚያደርገው በኒውክላር ሽክርክሪት እና በጠንካራ ውጫዊ የመግንጢሳዊ መስክ በሚደረግ እንተራክሽ ነው። ሁለት ጸባዮች መነምን ተግባራዊ ያደርጉታል። የመጀመርያው የኒውክላር ሽክርክሪት ላርመር ድግግሞሽ ባካባቢያዊው የመግንጢስ መስክ ላይ የተመረኮዘ መሆን ነው። ይህ እውነታ የ እያንዳንዱን ቲሹ ክፍል የመነም ሞገድ ለመለካት ይጥቅማል ። ይህን ለማድረግ ጠንካራ ና የማይለዋወጥ መግንጢሳዊ መስክ፣ በላርመር ድግግሞሽ የሚዋዥቅ መግንጢሳዊ መስክ እና ቦታን መሰረት አድርጎ የሚቀያየር መግንጢሳዊ መስክ መተግበር ያስፈጋል። ሁተኛው ጸባይ ደግሞ የቁአሚው ማግነታይዘሽ ክፋይ ማገገሚያ ጊዜ እና የ አግዳሚው ማግነታይዘሽን ክፋይ መክሰሚያ ጊዜ ለ ቲሹው ተፈጠሮ ስሜታዊ መሆን ነው። ይህ ደግሞ ከ ተለያዩ ቲሾች የተግኙትን ሞገዶች ለማውዳድር ይጠቅማል ። ይህ ጹሁፍ እነዚህን ጽንስ ሀሳቦች በጥልቅት ያብራራል።

Contents

1. Introduction

The objective of this essay is to describe the basic theoretical physics and techniques of magnetic resonance imaging (MRI).

One difficulty in the medical world is the limited knowledge about what is happening inside a patient's body. To overcome this problem much effort has been made and is still being made. The most powerful inventions resulting from this effort permit imaging the internal parts of the patient's body. This generates basic biomedical and anatomical information that provides new knowledge, and may allow early diagnosis of many diseases. The most common imaging techniques are MRI, X-rays and positron emission tomography (PET).

MRI is a medical diagnostic technique that combines strong magnetic fields usually about 1.5T, which is 30,000 times stronger than the earth's magnetic field, radio waves and computer technology to create images. It relies on the principles of nuclear magnetic resonance which concern signals emitted by spinning or rotating charged particles in a magnetic field. MRI can generate thin-section computerised images of any part of the body, including the heart's arteries and veins from any angle and in any direction [Par]. Unlike its X-ray counterpart, MRI does not require the passage of radiation through the imaged part; instead, it is the imaged organ that produces the signal.

In the case of X-rays, the technique is based on attenuation of the radiations as they pass through the sample, due to absorption of photons by electrons. Thus it is a matter of electron density that causes the difference in signal attenuation among tissues. This technique is not suitable for imaging soft tissues because of poor contrast and the absorbed photons may damage cells. However MRI is based on the relaxation signal emitted by excited nuclear spins in tissues placed in a strong magnetic field. The signal differences among tissues in the case of MRI are due to spin density, spin-lattice relaxation time (T_1) or spin-spin relaxation time (T_2) differences. MRI poses no known risk, except for patients who might have metals of high magnetic susceptibility in their bodies or electronic prosthetic devices such pacemakers.

MRI is possible in the human body because of the existence of small 'magnets' of hydrogen nuclei which are abundant. Whenever a spinning charge is exposed to an external magnetic field, its spin axis will precess about that field. This is like a spinning top in a gravitational field. The precession induces an electromagnetic signal; in the case of MRI this is a radio signal that can be detected by a radio antenna. Usually with imaging techniques the maximum signal is represented by white areas and the minimum signal is represented by black areas and any signal in between is represented by grey. Thus by showing signal contrast among tissues we are be able to image them.

In MRI imaging there are three types of magnetic fields that the object is exposed to. The first is the strong static magnetic field ($\overrightarrow{B_0}$) that causes net magnetisation of the body in one direction. The second is an oscillating or rotating field, called the RF-field, which is responsible for spin excitation of nuclei. The nuclei absorb photons only if the frequency of the photons is equal to their precession frequency. When this field is turned off the excited nuclei start to relax and emit photons of radio frequency. These photons in turn induce an electromagnetic signal in the coil

(antenna). The difficulty in MRI is localisation of the detected signal. The problem of localisation is overcome by applying the third type of magnetic field known as a gradient field.

A gradient field is a spatially linearly varying field with a certain gradient. To localise an MRI signal we apply three different gradient magnetic fields. These fields are directed along z-axis but their gradients are along x- and y- axes. The gradient magnetic field whose gradient is along z-axis is usually used to select a slice of a sample. However gradient magnetic field of gradients along x- and y- axes are used for frequency encoding and phase encoding respectively.

The essay is organised into three main sections:

In the first section, some fundamental physics principles are discussed. The relation of spins to nuclear magnetic dipoles, Zeemann energy levels, classical and quantum mechanical descriptions of the dynamics of the nucleus in an external magnetic field, induction of signals by a relaxation of precessing nuclei, and the essence of T_1 and T_2 are addressed.

In the second section the basic concepts of imaging are discussed. This section the details of slice selection, signal localisation, frequency encoding and phase encoding are described. We also examine some concepts of signal contrast, and T_1- and T_2-weighted images. There are some factors that distort images such as magnetic susceptibility, that causes magnetic field inhomogeneity across the sample, parts or whole motion of the sample, and aliasing that comes from sampling the continuous signal discretely. The general term for a distortion of an image is 'artefact'. This section devotes some pages to discuss the main sources of artefacts.

Finally in the third section, we summarise the most important concepts in MRI.

2. Basic physics of MRI

2.1 Classical magnetic dipole moment

From the fundamental physics of electromagnetism, we know that a charge experiences a magnetic force if it is moving in a magnetic field $\overrightarrow{B_0}$ at some angle θ to it; on the other hand a moving charge can also produce magnetic fields. Both of these facts are proved through experiments on a current-carrying wire. If we place a current-carrying loop in a magnetic field, it will rotate due to the torque exerted on it by the magnetic field. This torque is given by:

$$\overrightarrow{\tau} = I\overrightarrow{A} \times \overrightarrow{B_0}, \tag{2.1}$$

where I is the current and $\overrightarrow{A}$ is an area vector, whose magnitude is the area of the loop and whose direction is determined by the right-hand rule using the direction of the current circulation. The term $I\overrightarrow{A}$ is defined as the *magnetic dipole moment* of the loop, and it is denoted by $\overrightarrow{\mu}$. Hence the torque is given by

$$\overrightarrow{\tau} = \overrightarrow{\mu} \times \overrightarrow{B_0}. \tag{2.2}$$

A rotating, uniformly-charged sphere of charge q can be regarded as an infinite superposition of current loops. Detailed calculations give the resulting magnetic moment as

$$\overrightarrow{\mu} = \frac{q}{2m}\overrightarrow{L}, \tag{2.3}$$

where $\overrightarrow{L}$ is the angular momentum and m is mass of the sphere.

2.2 Quantum magnetic dipole moment of nuclear spin

The spin of a quantum particle is a fundamental property of nature like electrical charge or mass [Hor]. It behaves like an intrinsic angular momentum of constant magnitude. A particle of spin s $(= 0, \frac{1}{2}, 1, \frac{3}{2}, \ldots)$ has $2s + 1$ possible internal quantum spin states. These states are represented by $|s, s_z\rangle$, where s_z $(= -s, -s+1, \ldots, s)$ is spin magnetic quantum number. A particle with spin possesses a magnetic moment, just like a rotating charged body in classical physics. However $\overrightarrow{\mu} = \frac{q}{2m}\overrightarrow{L}$ does not hold. Instead the magnetic moment is entirely quantum mechanical in origin,and

$$\widehat{\overrightarrow{\mu}} = \gamma\widehat{\overrightarrow{S}}, \tag{2.4}$$

where γ is the gyromagnetic ratio, and $\widehat{\overrightarrow{S}}$ is the quantum spin operator. For example, for a hydrogen nucleus, $\gamma = 267.507$ MHz/T. The magnetic moment can be practically observed by the deflection of the particles in an inhomogeneous magnetic field. Two or more particles with spins having opposite signs can pair up to eliminate the observable manifestation of magnetic moment (spin). Thus a nucleus has a magnetic moment if either the protons or the neutrons are odd in number.

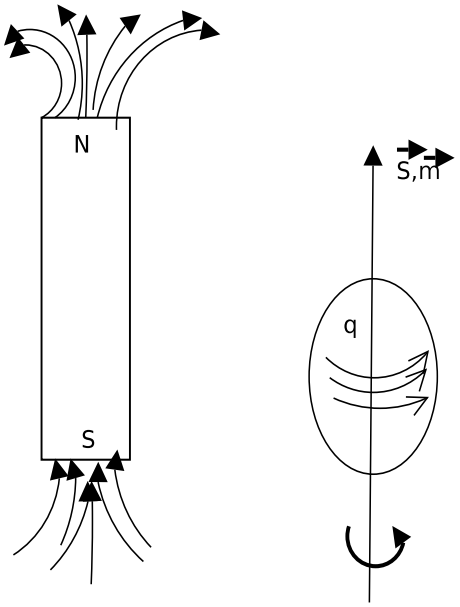

Figure 2.1: A spinning charge is like a magnet

2.3 Classical view of nuclear spins in external magnetic field

For clarification let us first review the motion of a top with angular momentum $\overrightarrow{L}$ in a gravitational field $\overrightarrow{g}$.

In figure 2.2 below, the force generated by the mass of the top and the gravitational acceleration ($\overrightarrow{F} = m\overrightarrow{g}$) appears to be acting at the centre of mass of the top, located at position $\overrightarrow{r}$, a distance r from the tip of the top. The simplified equation of motion for this top describes the torque on the top's angular momentum:

$$\overrightarrow{\tau} = \frac{d\overrightarrow{L}}{dt} = \overrightarrow{r} \times \overrightarrow{F}, \tag{2.5}$$

where $\overrightarrow{r} = r\hat{\mathrm{n}}$ and $\overrightarrow{L} = L\hat{\mathrm{n}}$, where $\hat{\mathrm{n}}$ is the unit vector along $\overrightarrow{L}$. This implies that $\overrightarrow{r} = r\frac{\overrightarrow{L}}{L}$. Hence

$$\frac{d\overrightarrow{L}}{dt} = \overrightarrow{L} \times \frac{rm}{L}\overrightarrow{g}.$$

The direction that the tip moves is perpendicular to the plane containing the axes of both $\overrightarrow{L}$ and $\overrightarrow{g}$. This is always true, and thus, as the position of the top changes, so does the direction of the movement. The path traced by the tip of the $\overrightarrow{L}$ vector forms a circle. This type of motion is known as *precession*. It can be easily shown that the precession frequency is given by $\Omega = \frac{rmg}{L}$ (in units of radians per second). The top precesses around the gravitational field at a rate proportional to the mass of the top, the strength of the gravitational field and the distance from the tip to the centre of mass. It is, however, inversely proportional to the angular momentum, which is related to the distribution of mass.

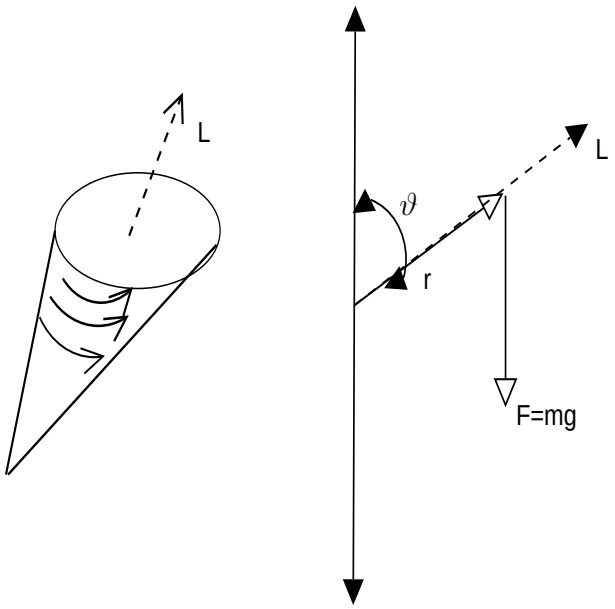

Figure 2.2: If a spinning top has sufficient spin angular momentum, it never falls down.

The classical description of a nuclear spin in a magnetic field is exactly the same as that of a top in a gravitational field. Since nuclear spins have an angular momentum, they do not snap to alignment with the magnetic field but they precess around it. The equation that describes this motion is :

$$\frac{d\overrightarrow{S}}{dt} = \overrightarrow{\mu} \times \overrightarrow{B_0}. \tag{2.6}$$

This implies that

$$\frac{d\overrightarrow{\mu}}{dt} = \gamma\overrightarrow{\mu} \times \overrightarrow{B_0} \tag{2.7}$$

since $\overrightarrow{S} = \frac{1}{\gamma}\overrightarrow{\mu}$. If the angle between $\overrightarrow{\mu}$ and $\overrightarrow{B_0}$ is θ,

$$\left|\frac{d\overrightarrow{\mu}}{dt}\right| = \gamma\mu B_0 \sin\theta. \tag{2.8}$$

This means the magnitude of the rate of change in $\overrightarrow{\mu}$ is constant, like the speed of a particle in uniform circular motion. Hence the tip of $\overrightarrow{\mu}$ moves around a circle of radius $\mu\sin(\theta)$ uniformly with speed $\gamma\mu B_0 \sin(\theta)$. For one complete rotation it takes $T = \frac{2\pi\mu\sin(\theta)}{\gamma\mu B_0 \sin(\theta)}$. Thus the angular frequency is $\omega_0 = \gamma B_0$. This relation is the most important one in MRI [Nol].

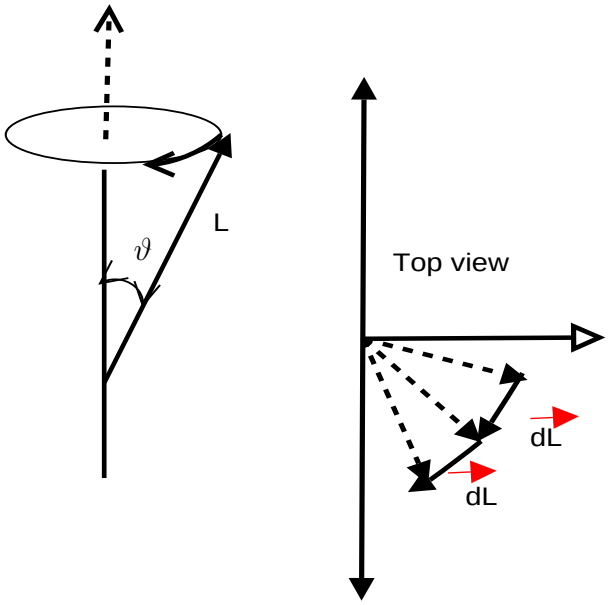

Figure 2.3: The precession of a spinning top traces a circle around the direction of gravitational field.

2.4 Quantum description of nuclear spin in an external magnetic field

In quantum mechanics physical observables are represented by Hermitian operators, and the dynamics of the system is described by Schrödinger equation as:

$$\frac{\partial|\varphi\rangle}{\partial t} = \frac{-i}{\hbar}\widehat{H}|\varphi\rangle, \tag{2.9}$$

where $|\varphi\rangle$ is the state vector of the system, $\hbar$ is the Planck constant (h) divided by 2π, and $\widehat{H}$ is the Hamiltonian of the system. For a nucleus in an external magnetic field $\overrightarrow{B_0}$, the Hamiltonian is given by

$$\widehat{H} = -\widehat{\overrightarrow{\mu}} \cdot \overrightarrow{B_0}, \tag{2.10}$$

where $\widehat{\overrightarrow{\mu}}$ is the magnetic moment given by equation 2.4. The expectation of the spin operator is given by

$$\langle\widehat{\overrightarrow{S}}\rangle = \langle\varphi|\widehat{\overrightarrow{S}}|\varphi\rangle. \tag{2.11}$$

Thus the dynamics of expectation of the spin is described by

$$\frac{d\langle\widehat{\overrightarrow{S}}\rangle}{dt} = \frac{d}{dt}\langle\varphi|\widehat{\overrightarrow{S}}|\varphi\rangle. \tag{2.12}$$

This implies that

$$\frac{d\langle\widehat{\overrightarrow{S}}\rangle}{dt} = \frac{i}{\hbar}\langle\varphi|\lceil\widehat{H}, \widehat{\overrightarrow{S}}\rceil|\varphi\rangle. \tag{2.13}$$

But

$$\lceil \widehat{H}, \widehat{S}_i \rceil = -\gamma B_j \lceil \widehat{S}_j, \widehat{S}_i \rceil$$

and

$$\lceil \widehat{S}_i, \widehat{S}_j \rceil = i\hbar\varepsilon_{ijk}\widehat{S}_k,$$

thus

$$\frac{d\langle \widehat{\overrightarrow{S}} \rangle}{dt} = \widehat{\overrightarrow{S}} \times \gamma \overrightarrow{B_0}. \tag{2.14}$$

This equation is exactly the same as the classical equation of precessing spin (magnetic moment) in a magnetic field.

Spin quantum states and nuclear energy levels are uniquely associated. The nuclear energy levels are collectively known as Zeemann energy levels [M.W03]. With no external magnetic field all spins are in the same energy level, i.e, they are indistinguishable. When spin$-\frac{1}{2}$ nuclei, however, are placed in an external magnetic field $\overrightarrow{B_0}$ along the z-axis, they will tend to align either with, or opposite to the direction of the applied field. These two states are called 'spin-up' and 'spin-down' respectively. The spin-up state is at lower energy relative to the spin-down state as we can see in equation 2.10. Thus under normal laboratory conditions there is slight excess of spin-up over spin down states. The energy level of a nucleus in a magnetic field is given by equation 2.10 as

$$E = -\overrightarrow{\mu} \cdot \overrightarrow{B_0}. \tag{2.15}$$

If the external field is applied along the z-axis and the z-component magnetic moment is $\mu_z = \gamma\hbar s_z$ then the spin energy is therefore given by $E = -\gamma\hbar B_0 s_z$. This equation shows that the magnetic field affects the energy levels but not the distribution of spins in the energy levels. The distribution is always affected by s_z which is an inherent property of the nuclei. The nucleus absorbs energy which is equal to the energy difference between two consecutive energy levels so that it jumps from the lower to the upper energy level (excited). This will be achieved only if the nucleus absorbs a photon with the required energy. The energy of a photon with frequency ν is given by:

$$E_p = h\nu, \tag{2.16}$$

so the necessary photon frequency required to jump the nucleus from s_{z0} to s_{zf} is derived from

$$h\nu_0 = \gamma\hbar B_0(s_{zf} - s_{z0}) \tag{2.17}$$

and

$$h\nu_0 = \gamma\hbar B_0 \tag{2.18}$$

as

$$\omega_0 = \gamma B_0. \tag{2.19}$$

This expression is exactly the same as that of the classical expression of the Larmor frequency.

The spins and the associated magnetic moments are probabilistic in nature in the same way as electrons surrounding the nucleus travel in probabilistic volumes or shells. Thus each spin does

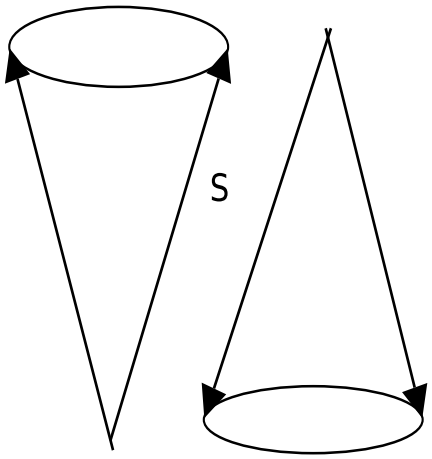

Figure 2.4: Spin-up and spin-down cones

not align with $\overrightarrow{B_0}$, but rather exists in a probabilistic cone. Spin-up and spin-down imply that the probabilistic cone faces either up or down.

The spin and magnetic moment exist simultaneously but expectation is non-zero only in the direction of the magnetic field: $\langle \mu_x \rangle = \langle \mu_y \rangle = 0$ but $\langle \mu_z \rangle = \hbar \gamma s_z$. Here the basic question is, what is the population distribution of nuclei in these two energy states, and how many extra nuclei are there in the lower energy state? These are governed by the thermal equilibrium condition, which is characterised by the Boltzmann distribution. Let N_+ and N_- be the number of nuclei in the higher (spin-up) and lower (spin-down) states respectively. The Boltzmann distribution dictates that:

$$\frac{N_+}{N_-} = \exp(\frac{-\Delta E}{kT}), \tag{2.20}$$

where k is the Boltzmann constant (8.62×10^{-5} ev/K or 1.38×10^{-32}J/K), T is the temperature of the system in kelvin (K), and ΔE is the energy difference of the two states equal to $\hbar \gamma B_o$. But $\frac{\Delta E}{kT}$ is very small, thus using the first two terms of Taylor series expansion of exponent we get

$$\frac{N_+}{N_-} = 1 - \frac{\Delta E}{kT}, \tag{2.21}$$

and $\Delta N = \frac{\Delta E}{kT} N_- = \frac{\hbar \gamma B_0}{kT} N_-$. Thus ΔN is proportional to γB_0.
The net magnetic moment is defined as $\overrightarrow{m} = \Delta N \langle \overrightarrow{\mu} \rangle$ and the magnetisation ($\overrightarrow{M}$) of the system is the net magnetic moment per unit volume.

$$\overrightarrow{M} = \frac{\overrightarrow{m}}{V}. \tag{2.22}$$

These excess spin-up nuclei are the source of magnetisation for all MRI experiments [Nol]. It follows then that a large magnetic field $\overrightarrow{B_0}$ will generate a large magnetisation to perform our imaging experiments. From equation 2.7 and the definition of magnetisation, it is straightforward to show that the dynamics of magnetisation ($\overrightarrow{M}$) in an external magnetic field ($\overrightarrow{B_o}$) is described by the equation

$$\frac{d\overrightarrow{M}}{dt} = \overrightarrow{M} \times \gamma \overrightarrow{B_0}. \tag{2.23}$$

This is known as the Bloch equation. The Bloch equation says that the magnetisation will precess about the external magnetic field at a frequency $\omega_0 = \gamma B_0$. Now let $\overrightarrow{M}$ lie in a plane perpendicular to the magnetic field along the z-axis. For this system $\overrightarrow{M}$ will precess in the x-y plane at a frequency $\omega_0 = \gamma B_0$ as shown in figure 2.5.

If we place a small loop of wire near this precessing magnetisation an electromotive force $V(t)$ will be induced in the coil at the frequency γB_0. This induction of voltage in the coil from precession of the magnetisation in the x-y plane is the basis of signal reception in MRI [Nol].

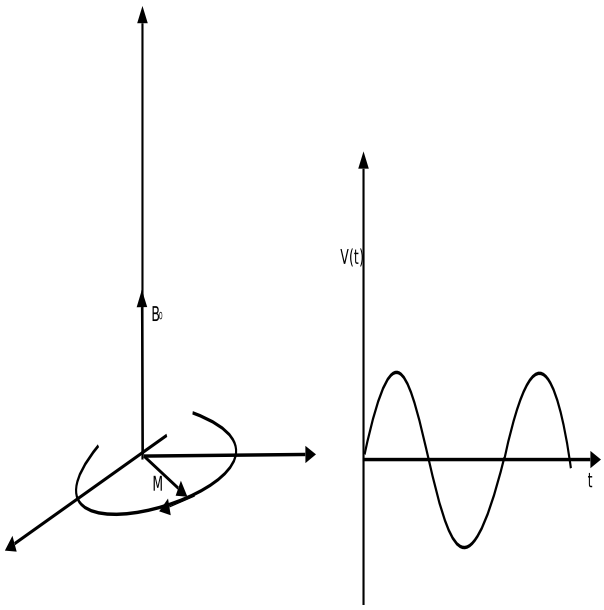

Figure 2.5: A precessing magnetisation induces a time-dependent electric voltage

2.5 Rotating magnetic field and excitation in MRI

So far we have only been discussing spin in the static external magnetic field $\overrightarrow{B_0}$. In MRI, this is known as the main magnetic field [M.W03]. It a very strong field. Now we are in the position to discuss another type of important external magnetic field known as $\overrightarrow{B_1}$. $\overrightarrow{B_1}$ is a magnetic field which rotates with Larmor frequency. The Larmor frequency is in the range of radio frequency, so $\overrightarrow{B_1}$ is called an RF-field. This field is applied in the plane transversal to $\overrightarrow{B_0}$. The total external field in which $\overrightarrow{M}$ is placed will now be

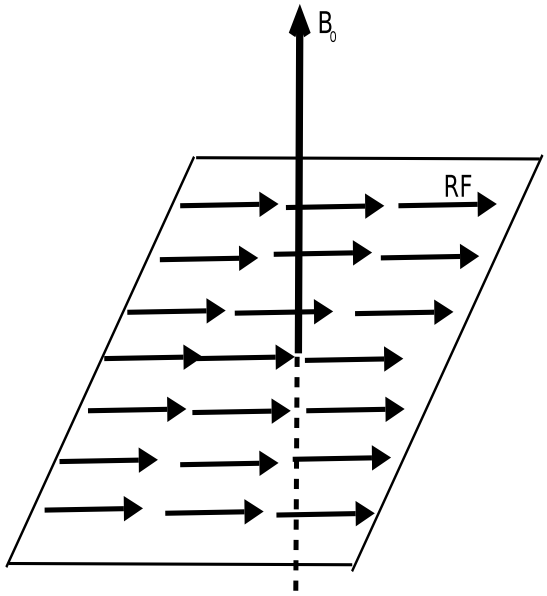

Figure 2.6: Static longitudinal and rotating transversal magnetic filed

$$\overrightarrow{B} = \overrightarrow{B_0} + \overrightarrow{B_1}. \tag{2.24}$$

Since $\overrightarrow{B_1}$ is a rotating field, $\overrightarrow{B}$ is also rotating;

$$\begin{bmatrix} B_x \\ B_y \\ B_z \end{bmatrix} = \begin{bmatrix} B_1 \cos(\omega_0 t) \\ B_1 \sin(\omega_0 t) \\ B_0 \end{bmatrix}. \tag{2.25}$$

Thus the magnetisation will precess about a rotating axis directed along $\overrightarrow{B}$. Equation 2.23 becomes

$$\frac{d\overrightarrow{M}}{dt} = \overrightarrow{M} \times \gamma(\overrightarrow{B_0} + \overrightarrow{B_1}). \tag{2.26}$$

Hence the angular velocity will be $\overrightarrow{\omega} = \overrightarrow{\omega_0} + \overrightarrow{\omega_1}$, where $\omega_1 = \gamma B_1$. If $\overrightarrow{B_1}$ is applied for a time interval T, the magnetisation will be tipped by an angle $\theta = \omega_1 T$ from the z-axis. So by applying $\overrightarrow{B_1}$ for the appropriate time interval, it is possible to tip the magnetisation to the desired angle, even up to inversion ($\theta = 180^o$) of the magnetisation. If $\theta = \frac{\pi}{2}$ the applied pulse is known as a 90^o pulse. Similarly, a 180^o pulse is one that rotates $\overrightarrow{M}$ through 180^o degrees.

The quantum-mechanical interpretation is that if the RF field is applied, the nuclei will be excited by absorbing photons of energy equal to the energy difference between two consecutive spin states. However, they will absorb energy only if the frequency of the photon is exactly the same as the Larmor frequency. This frequency-selective behavoiur is known as *resonance*.

2.6 Relaxation process

When the tipping field $\overrightarrow{B_1}$ is removed (turned off), the distribution of the spin energies will start to revert to the distribution when no tipping field was imposed. The longitudinal magnetisation will recover simultaneously with the decay of the transversal magnetisation by emitting photons. Classically the magnetisation rotates back to the z-axis - the longitudinal component will increase and the transversal will decrease. This process resembles the decay of one nucleus and creation of another that occurs in a radioactive process. However, the rate of recovery of the longitudinal magnetisation is not the same as rate of decay of the transversal magnetisation. Specifically, the equations that describe these dynamics are given by:

$$\frac{dM_z}{dt} = -\frac{1}{T_1}(M_z - M_0) \tag{2.27}$$

and

$$\frac{dM_{xy}}{dt} = -\frac{1}{T_2}M_{xy}. \tag{2.28}$$

where $\frac{1}{T_1}$ and $\frac{1}{T_2}$ are the rate constants of the longitudinal recovery and transversal decay of magnetisation respectively. These equations have solutions

$$M_z = M_0 + (M_z(0) - M_0)\exp(-t/T_1) \tag{2.29}$$

and

$$M_{xy} = M_{xy}(0)\exp(-t/T_2). \tag{2.30}$$

The relaxation processes are characterised by the values of T_1 and T_2, i.e. the times for full recovery of M_z and complete decay of M_{xy} are determined by T_1 and T_2 respectively. By measuring the signal induced in the RF coil by the emitted photons during relaxation for certain intervals, it is possible to determine the values of T_1 and T_2 experimentally.

Experimental measurement of T_1 and T_2

To determine T_1, first we apply a tipping field with a strength capable of tipping the magnetisation to the desired angle. This angle is unrestricted in principle, but in general the accuracy of the T_1 measurement will increase as the initial tipping angle approaches π radians, requiring a longer scanning sequence [M.W03]. 180^o tipping is called inversion recovery. Another important initial tipping angle is 90^o and it is known as saturation recovery. Then starting from the removal of the tipping field, we read the strength of the net longitudinal magnetisation for a long sequence of time intervals. We can do this using the RF-coil. However the coil will detect the signal only if its plane is perpendicular to the magnetisation. Thus to detect the signal with the RF-coil, we should first rotate the magnetisation by $\frac{\pi}{2}$ radians. The time between the initial tipping pulse and the $\frac{\pi}{2}$ tipping pulse required to generate the signal may be increased in a series of successive scans [M.W03]. Then we apply curve fitting techniques to calculate the value of T_1 from the data we collected. This is easy because we know the values of $M_z(0)$ and M_0 of equation (2.29) and it is exponential curve fitting [Hug91]. For the following experimental data, we can simply

use least square fitting and find that T_1 is 150.0 $+$1.99ms (-1.93ms), where the last values are the limits of the 95% confidence interval.

Times in ms	5	10	20	40	80	160	320	640	960	1280
Magnetisation	-46429	-43663	-37514	-26509	-8685	15544	38347	47979	49781	50424

Table 2.1: Experimentally measured values of magnetisation along the static field $\mathbf{B}_0$ through series of time intervals during relaxation to determine T_1.

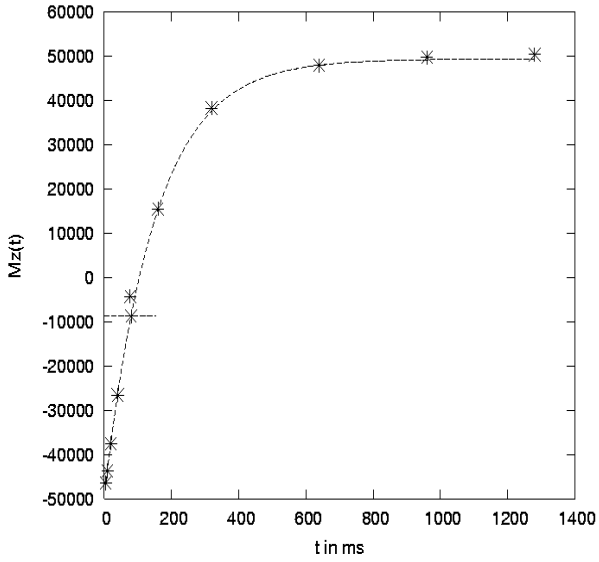

Figure 2.7: Longitudinal magnetisation inversion recovery through time.

T_1 and T_2 are often affected by the same relaxation mechanisms. In particular any chemical or process that shortens T_1 must also shorten T_2, although the converse is not true [VBea96]. One of the factors that affects T_2 but not T_1 is dephasing of the nuclear spins. It is caused by the inherent electromagnetic property of our sample and inhomogeneity of the external static field. However the latter is not included in measurement of T_2 because it depends on the machine that produces the field.

It is impractical to produce an absolutely uniform magnetic field to permit proper T_2 values to be ascertained directly from the magnetisation after it has been tipped through 90^o. However if the magnetisation is tipped by 180^o after a 90^o pulse, the effect is the same as if the polarity but not the strength of $\overrightarrow{B_0}$ had been reversed. The dipoles will precess in the reverse direction thus they rephase instead of dephasing. Hence the signal increases to a peak. After the instance of the signal peaking it starts to decrease since they again start dephasing. Although the rephased peak signal is generated directly from the precessing dipoles, it is termed an "echo". The 90^o -180^o tipping sequence is called a spin - echo sequence [M.W03].

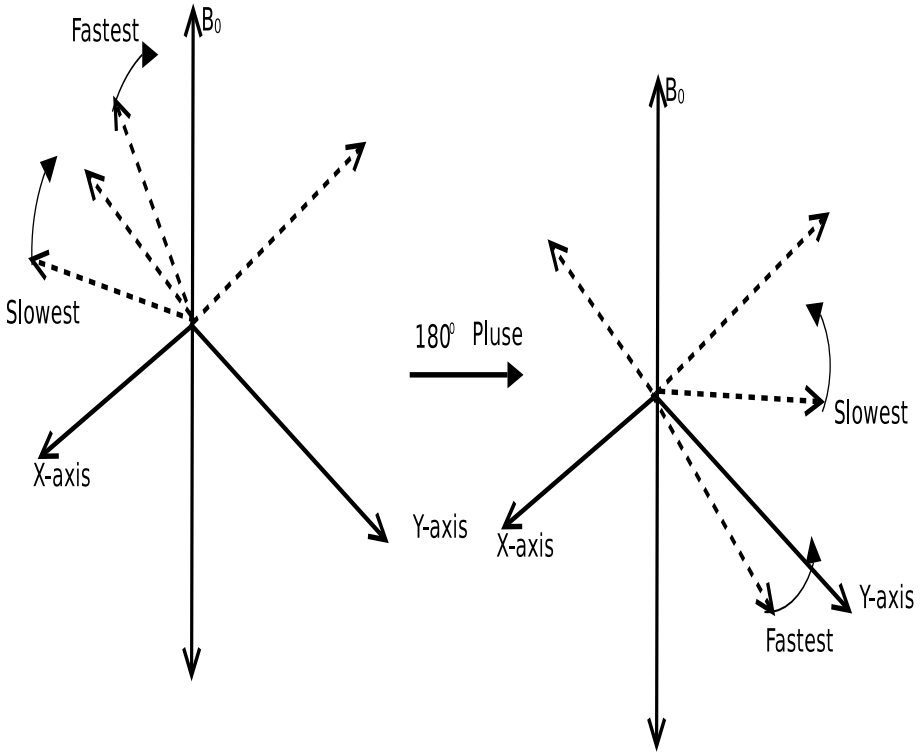

Figure 2.8: Spin echo is created by the application of 180^o pulse

Time in ms	1	2	3	4	5	6	7	8	9	10	11	12
Magnetisation	42935	35987	30781	25434	21744	18483	15476	12968	11024	9322	8069	6797
Time in ms	13	14	15	16	17	18	19	20	21	22	23	24
Magnetisation	5595	4819	4000	3454	2907	2349	2052	1870	1566	1231	1081	965
Time in ms	24	25	26	27	28	29	30	31	32	33	34	36
Magnetisation	697	684	513	477	442	335	282	240	239	172	152	134
Time in ms	37	38	39	40	41	42	43	44	45	46	47	48
Magnetisation	129	93	61	52	35	47	22	43	14	25	23	27
Time in ms	49	50	51	52	53	54	56	57	58	59	60	61
Magnetisation	9	16	5	16	7	7	6	2	9	0	7	4

Table 2.2: Experimentally-measured values of magnetisation transversal to the static field $\mathbf{B}_0$ through a series of time intervals during relaxation to determine T_2.

The value of T_2 determined from the above table using least square fitting is $5.9966{+}1.20$ms$(-0.135$ms$)$, where the last values are the limit of the 95% confidence interval.

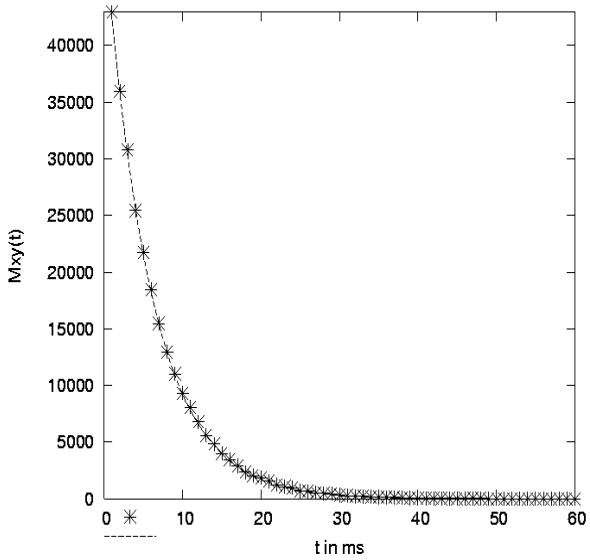

Figure 2.9: Transversal magnetisation decay through time.

3. Magnetic resonance imaging (MRI)

3.1 Signal localisation

One advantage of MRI is that T_1 and T_2 are very sensitive not only to small differences in the type of substances, but also to small differences in the proportion of the chemicals of which tissue is composed. If we can measure T_1 and T_2 for each part of the tissue, we can map them into an image of the tissue. Unfortunately we cannot measure them for every part because the RF coil measures the signal coming from the whole tissue that is undergoing relaxation.

However, MRI is made possible because the precession frequency of the tipped nuclei depends on the external magnetic field. The signal in the RF coil in turn reflects the precession frequency of the spins. The magnetic field, the Larmor frequency and the induced signal are uniquely associated. Thus we can induce a position-dependent frequency and signal by applying a position-dependent magnetic field. In order to know specifically the signal produced by each part, we should convert the time domain signal to a frequency domain. To do so, we can use a Fourier transform. The Fourier transform of a signal $s(t)$ is given by:

$$S(\omega) = \int_{-\infty}^{\infty} s(t) \exp(-i\omega t)\, dt. \tag{3.1}$$

For a specific variation of the magnetic field across the sample, we must apply a spatially-varying field with a particular gradient. This magnetic field is known as a *gradient magnetic field*. In principle this gradient can be applied in any direction, but for practical purposes it is applied along the x-,y- and/or z-axes. The problem is that each gradient encoding now represents all nuclear spins along the isomagnetic contours, not points along the contours. For example if the gradient is along the x-axis, all the dipoles lying along the isomagnetic contour perpendicular to the x-axis precess with the same frequency. Thus we cannot measure signals of every point of the sample along the isomagnetic contours. This problem cannot be surmounted by applying another gradient magnetic field along the contour simultaneously, since that would create another isomagnetic contour perpendicular to the resultant vector of the two gradient fields. To solve this problem, we use frequency encoding in one dimension and phase encoding in another dimension.

3.2 Slice selection

When the excited nuclei relax, they emit photons of radio frequency. These photons induce an electromagnetic signal in a coil called the radio antenna.

At any instant, the signal detected by the coil is the sum of the signals produced by all relaxing parts of the specimen. In order for us to contrast the MRI image, we need to calculate the relative strengths of the signals originating from different parts of the specimen. The first task will be to select a slice of the specimen. This can be done by applying a gradient field along the z-axis and

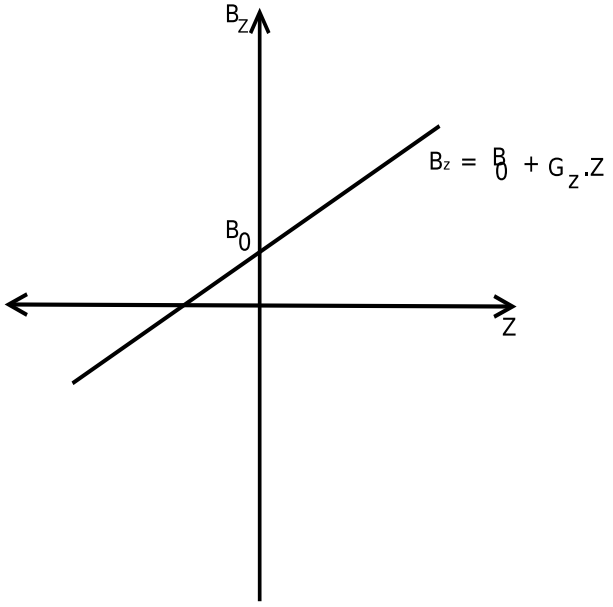

Figure 3.1: Graph of the external magnetic field versus z where the gradient is along z-axis.

a sinc RF pulse in the transversal plane to the z-axis. The sinc pulse is defined as

$$\text{sinc}(\omega_0 t) = \begin{cases} 1 & \text{if } \omega_0 t = 0 \\ \frac{\sin(\omega_0 t)}{\omega_0 t} & \text{otherwise.} \end{cases}$$

Its Fourier transform is a rectangular function of a certain band of frequencies.

When the z-gradient is applied in such a way that the gradient is symmetric about the mid-plane of the sample, the nuclei above this plane precess faster while the nuclei below the plane precess more slowly. If with this gradient field switched on, an RF pulse of a single band of frequencies is applied to the whole sample, only nuclei in the middle plane, perpendicular to the longitudinal and whose frequencies are in this band will absorb the RF energy. Everywhere else in the sample, nuclei receive the wrong frequency of excitation for resonance to occur [M.P]. Thus the signal detected by the antenna comes from the relaxing spins in the excited slice only. The size of the slice will be determined by the gradient. Now the question will be, how can we resolve individual points of the selected slice?

3.3 Frequency encoding

If the slice is in a magnetic gradient along the x-axis during signal detection, the frequency of all nuclei along an isomagnetic contour perpendicular to the gradient is different from any other isomagnetic contour since

$$\omega(x) = \omega_0 + \gamma G_x x. \tag{3.2}$$

Hence the frequencies of the photons emitted by the relaxing nuclei spins are directly related to their location along the gradient. This relation is called *frequency encoding*. The signal we detect will be in the time domain.

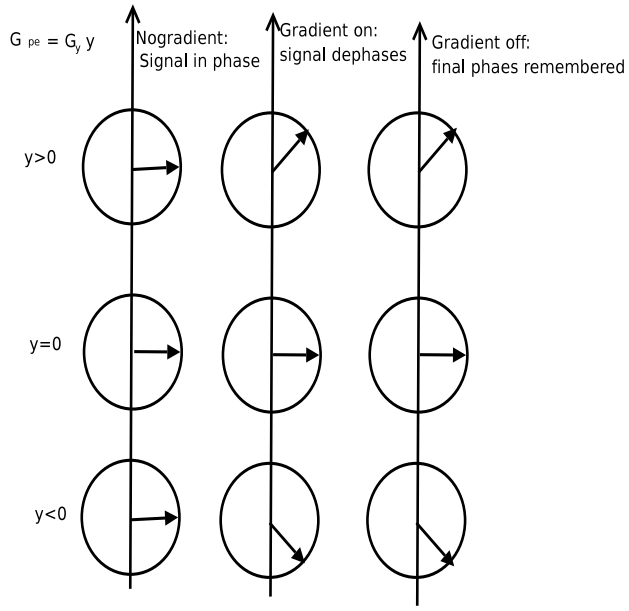

Figure 3.2: Phase encoding returns the signal to the Larmor frequency but with position dependent phase changes.

By taking the Fourier transform, we can determine the signal induced by nuclei precessing with in certain bands of frequencies. These bands of frequencies correspond to strips of the slice.

3.4 Phase encoding

The frequency encoding enables us to measure the signal induced by each strip of the slice. But this is not enough to construct the image of the slice. To do that, we need to know the signal induced by each volume element of the strip, called a *voxel*. We apply another gradient along the strip (y-axis) for an interval of time t_p. During this time, nuclei along the gradient will precess with different frequencies,

$$\omega(y) = \omega_0 + \gamma G_y y. \tag{3.3}$$

As shown in figure 3.2, this frequency difference results in a phase angle difference even after the gradient is turned off. When we turn off the gradient the frequency reverts to its initial value before the gradient was imposed but with the phase difference retained. There is a difference between the signal induced by a strip before the gradient is imposed and after the gradient is turned off. This is due to the phase shift of nuclei across the strip resulting from the gradient. If we increase the gradient or the time interval t_p more nuclei will be out of phase so that the signal reduces more and finally become zero, i.e. the signal produced by all nuclei cancels each other.

While the frequency encoding magnetic gradient is applied, the signal induced by the whole slice corresponds to a frequency band $[F]$. If we divide the slice into n equal sized strips, each strip $'i'$ will have its own frequency band $[f_i]$. After the phase encoding gradient is turned off there will be a phase shift among the signals produced by the voxels, since the nuclei in the voxels are

at different phase angles. To measure every voxel signal of n by n slice we need to measure the slice signal n times by applying n different phase encoding gradients. Let 'i' and 'j' denote the strip and the voxel respectively. For no-phase shifting magnetic gradient, the signal induced by strip 'i' is then given by:

$$S_iG_1 = A_1\sin(\omega t) + A_2\sin(\omega t) + A_3\sin(\omega t) + A_4\sin(\omega t) + ... + A_n\sin(\omega t).$$

For a first-phase shifting magnetic gradient we have

$$S_iG_2 = A_1\sin(\omega t+\phi_{12})+A_2\sin(\omega t+\phi_{22})+A_3\sin(\omega t+\phi_{32})+A_4\sin(\omega t+\phi_{42})+...+A_n\sin(\omega t+\phi_{n2}).$$

Similarly for the second-phase shifting magnetic gradient

$$S_iG_3 = A_1\sin(\omega t+\phi_{13})+A_2\sin(\omega t+\phi_{23})+A_3\sin(\omega t+\phi_{33})+A_4\sin(\omega t+\phi_{43})+...+A_n\sin(\omega t+\phi_{n3})$$

.
.
.

and finally for the $(n-1)^{th}$-phase shifting magnetic gradient

$$S_iG_n = \Sigma_{j=1}^{n} S_{ij}$$

where $S_{ij} = A_j\sin(\omega t + \phi_{jn})$ is the signal from voxel ij. A_j's are unknown amplitudes. They do not depend on the strength of the gradient. They are an intrinsic property of the voxels. The phase shift ϕ_{jn}'s can be calculated from the gradient and t_p. Theoretically we have n equations with n unknowns so by certain computer codes we can solve them and determine the signal emitted by each voxel.

S_{11}	S_{12}	S_{13}	S_{14}	S_{15}
S_{21}	S_{22}	S_{23}	S_{24}	S_{25}
S_{31}	S_{32}	S_{33}	S_{34}	S_{35}
S_{41}	S_{42}	S_{43}	S_{44}	S_{45}
S_{51}	S_{52}	S_{53}	S_{54}	S_{55}

Table 3.1: Signals produced by voxels along different strips, when the frequency encoding is the horizontal and the phase encoding is the vertical

However, theory and practice are often different. Due to imperfections in the homogeneity of the static magnetic field $\overrightarrow{B_0}$, there is actually a difference in the value of ω among the voxels. We cannot determine the gradient precisely so our knowledge of the values of the phase shift are not completely reliable. Hence the solution for the amplitudes are affected by these inaccuracies.

To minimise the inaccuracy in our solution, we apply the concept of spatial frequency. The spatial frequency of a given event is defined as cycle of its appearance per unit of space, instead of per

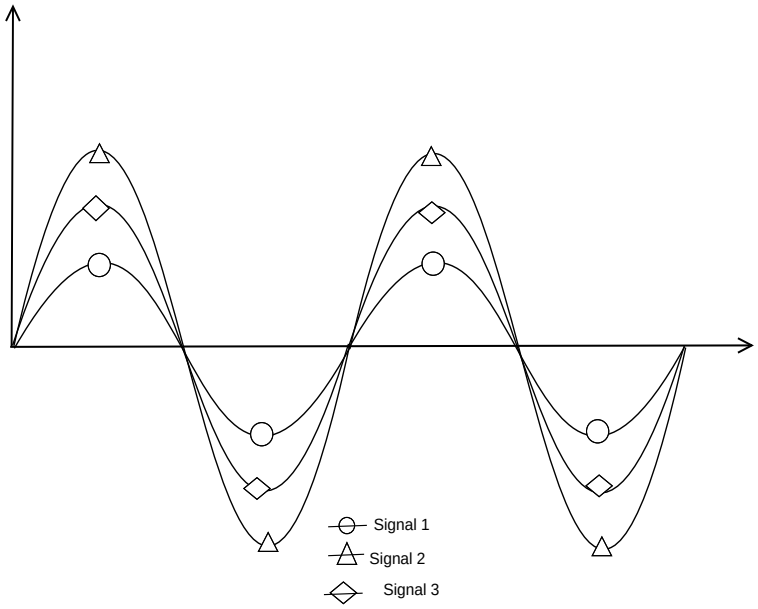

Figure 3.3: Three signals emitted by different voxels when there is no gradient field.

unit time. One of the easiest ways of understanding spatial frequencies is to think of line-pairs. These consist of alternate light and dark bands, or line-pairs, of differing space. Suppose we have five line-pairs per centimetre. This means that five dark-light patterns are contained in a single centimetre. The pattern of image brightness produced by these line-pair patterns is like a spatial frequency. In MRI a spatial frequency is a periodic variation in a signal distribution or image brightness, measured not in line-pairs per centimetre, but rather in cycles per centimetre (which are very similar) [MMGP03].

From wave physics we know that two waves with phase difference $2\pi n$ $(n \epsilon N)$ interfere in such a way that all the peaks line up with the peaks and the troughs line up with the troughs. Thus the amplitude of the resulting wave is larger than the individual amplitudes.

Let us consider the signal induced by strip i when the first phase shift gradient is applied. We can design the scanner in such a way that the gradient should create a $2\pi n$ phase shift among signals of certain voxels in the strip. This shift could occur at equally spaced intervals. For example if each voxel has a $2\pi n$ phase shift with respect to the sixth voxel to either side, and if there are about 25 voxels in each centimetre, there will be a single $2\pi n$ phase shift within 2mm.

We can model this situation using spatial frequency. The interesting thing here is that by changing the gradient we can change the size of the interval over which $2\pi n$ the phase shift appears. Thus for n different gradients, we obtain n different signals each with a different spatial frequency. By taking the Fourier transform of the sum of all these signals we can convert from the frequency domain to the space domain, and associate the signal strength with the location of voxels.

In imaging, the maximum and minimum signals are typically represented by white and black respectively. Intermediate signals are represented by appropriate shades of grey.

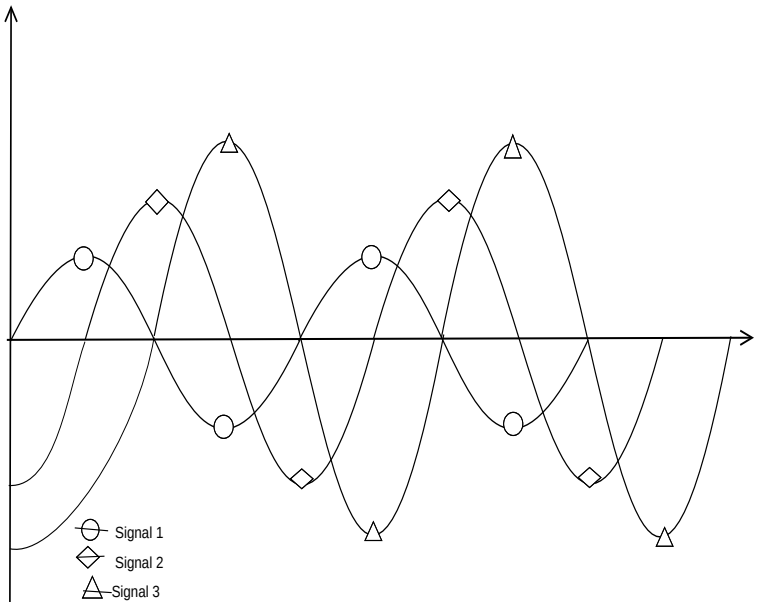

Figure 3.4: Three signals induced by different voxels after a gradient field has been imposed for a finite time.

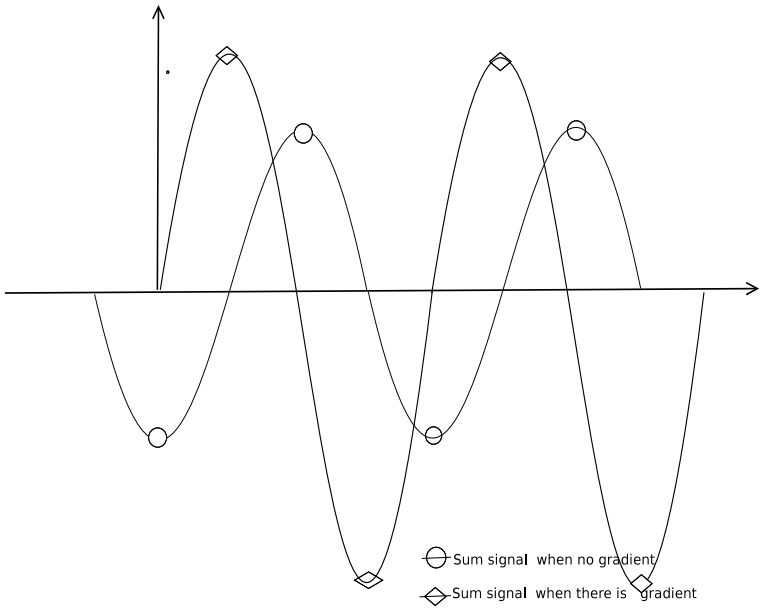

Figure 3.5: The summed signal from the three voxels after a gradient field is less than its counterpart when there is no field gradient

3.5 k-space

We now introduce the concept of k-space, a 'temporary image space' in which the digitised signal is stored during signal acquisition. It is a space filled by numbers that represent acquired signals. The k-space contains a lot of information about the real space in an encoded form. Its size is determined by the number of pixels along the frequency and phase encoding axes. For example if the frequency encoding axis contains 256 pixels, the k-space will have 256 columns; and if the number of pixels along the phase encoding axis is 256, the rows in the k-space will be 256. However the information contained in k-space is not directly related to real space. For example the information at one point of k-space does not represent the same position in real space. This is due to the Fourier transform of the signal to reconstruct the image [MMGP03]. The data in the middel of the k-space are for low spatial frequencies and provide image contrast, whereas the surrounding data are for high spatial frquencies corresponding with boundaries and edges. The former has a high signal-to-noise ratio while the latter has a low signal-noise ratio.

3.6 Signal contrast between tissue types

To distinguish between two tissues in MRI, we use signal contrast. The signal from region of tissue depends on its intrinsic properties: proton density (PD), T_1 and T_2 and sequence parameters like tipping pulse, repetition time (TR) and echo time (TE). The tipping pulse may be either 90^o or $\alpha < 90^o$. If the tipping pulse is 90^o and the echo is created by another 180^o pulse at TE/2, the sequence is called a *spin echo* (SE); whereas if the pulse is $\alpha < 90^o$ and the echo is created by changing the sign of the gradient from positive to negative at TE/2, it is called a *gradient echo* (GE). TR is defined as the time between two consecutive tipping-pulses, the time from one 90^o pulse to the next 90^o in SE. Similarly in GE, TR is the time from one α pulse to the next α. TE is the time from the action of the tipping pulse to the time of echo in both sequences.

Even if these three intrinsic properties of a tissue affect its signal, it is possible to suppress two of them and leave the signal depending on only one of them through controlling the sequence parameters. An image whose signal contrast depends mainly on T_1 is known as a T_1-weighted image. Similarly image whose contrast depends mainly on T_2 is called a T_2-weighted image. The same is true for PD-weighted images.

3.7 T_1-weighted image

We can construct a T_1-weighted image using either an SE or a GE sequence. However, here we focus on SE. We need to use short TR and short TE ($<$ 40ms) to enhance the T_1 difference between tissues. If we wait only a short time after tipping the longitudinal magnetisation before measuring the signal, then the difference in longitudinal magnetisation between tissues due to T_1 difference will be large. However if a longer time is allowed to pass, the difference in longitudinal magnetisation between tissues due to T_1 will be small. Thus short TR (400ms $<$ TR $<$ 750ms)

enhances the differences in signals arising from differences in T_1 of tissues even though longer TR would provide more longitudinal magnetisation for both tissues. This is clearly seen in figure 3.6a.

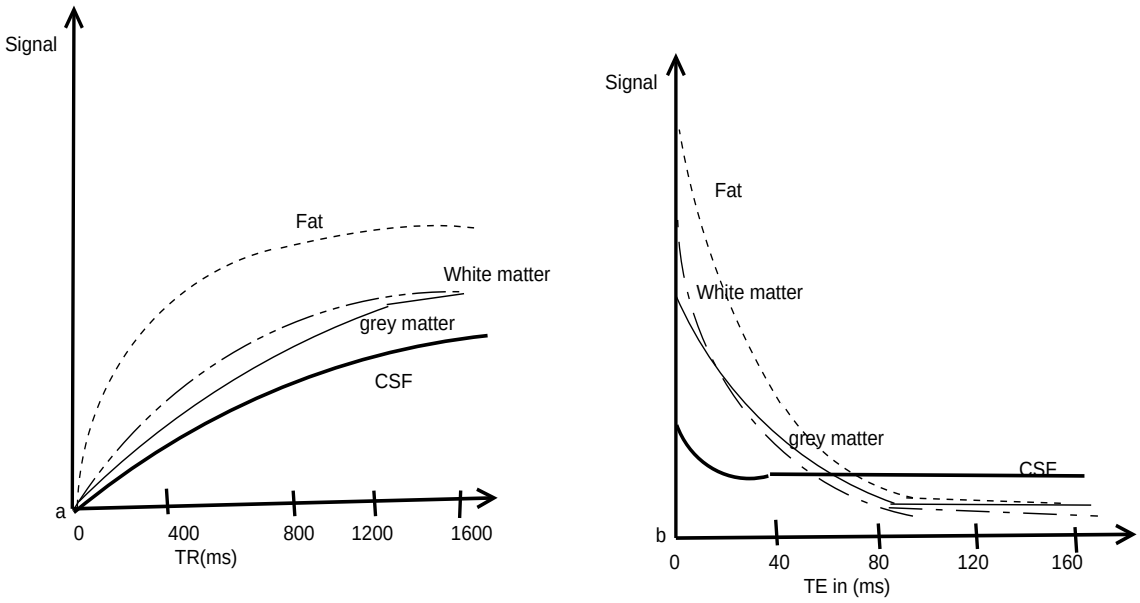

Figure 3.6: a) T_1 contrast of signals of brain tissues. b) T_2 contrast of signals of brain tissues.

3.8 T_2-weighted image

In this case we need to make TR long so that the longitudinal magnetisation is almost fully recovered and the next tipping provides maximum transversal magnetisation. We can use either an SE or GE sequence, but in the case of GE we do not have real T_2 contrast rather we will have an apparent relaxation time called T_2^*. This is due to the inhomogeneity of the static field. If we wait for a short time before measuring the signal (TE is short), the difference in transversal magnetisation between tissues due to the T_2 difference will be small. Thus for short TE the signal difference between tissues due to the T_2 difference is small. However, if TE is long the difference in signals between tissues arising from the T_2 difference will be large since the transversal magnetisation difference due to T_2 is large even if the transversal magnetisation of both tissues are small. Thus we need long TE ($>$ 30ms) to enhance the signal differences between tissues that arise from their T_2 differences. Figure 3.6b shows this. In a T_2-weighted image, contrary to a T_1-weighted image, tissues of long T_2 are bright and tissues of short T_2 are dark.

3.9 Artefacts in MRI

1. The term 'artefact' refers to the occurrence of undesired image distortion, which can lead to misinterpretation of MRI data [M.P].

2. Artefacts in MRI can be most generally defined as any image content that does not correspond to the actual object distribution or random noise [Nay].

From these two equivalent statements, we can understand that artefacts are errors in imaging. In MRI there are different factors that distort the image such as magnetic susceptibility of the tissue, aliasing, motion (part or whole motion of the patient or the scanner) and signal from external sources. Here we focus on the problem created by magnetic susceptibility and aliasing.

According to their magnetic susceptibility substances can be grouped in to diamagnetic, paramagnetic or ferromagnetic [Ser90].

- A diamagnetic material is a substance whose magnetic susceptibility χ is negative so that the magnetisation is in the opposite direction to the external magnetic field and the net magnetic field in the material is less than the applied external magnetic field.
- A paramagnetic material is a substance whose magnetic susceptibility χ is positive so that the magnetisation is aligned with the external magnetic field and the net magnetic field in the material is stronger than the applied magnetic field.
- In the case of ferromagnetic materials, the magnetic susceptibility is positive like a paramagnetic material but it is much biger.

Thus magnetic susceptibility differences affect the magnetic field homogeneity across a sample. For example, if the sample is made of diamagnetic and paramagnetic substances, the magnetic field in the paramagnetic part is stronger than that of the diamagnetic part. This causes dephasing that shortens T_2^* so that signal will be either weak or zero. Magnetic susceptibility greatly affects the signal when we use GE. This problem can be reduced by using a shimming magnet.

Nyquist Theorem

Analog-to-digital converters use sampling, i.e. they measure the intensity of the signal at discrete sample points at equal time interval. However a digital-to-analog converter uses an interpolator to reproduce the original signal. The number of sampling points per unit time is known as sampling rate or frequency. Any analog signal can be viewed via a Fourier transfom as being made up of components of different frequencies. The highest frequency component of the analog signal is known as the *bandwidth* of the signal. For good reproduction of the analog signal from the digital signal, the Nyquist criterion must be fulfilled. The Nyquist theorem states that if the maximum frequency of the analog signal is f_{max}, the sampling rate must be greater than $2f_{max}$ in order to reproduce the analog signal correctly [A.P77]. If the rate is less than $2f_{max}$, when the output digital signal is converted back to analog form by the digital-to-analog converter false frequency components will appear that were not in the original analog signal. This undesirable condition is a form of distortion called *aliasing*

For mathematical clarification of the concept of Nyquist theorem, let us consider a given signal $x(t)$ with Fourier transform $X(\omega)$, where $X(\omega)$ is zero outside a range $\frac{-\pi}{T} < \omega < \frac{\pi}{T}$. T is the

sampling interval so that the sampling frequency as required by the Nyquist theroem is $\frac{2\pi}{T}$. $x(t)$ is related to X by an inverse Fourier transform,

$$x(t) = \frac{1}{2\pi}\int_{-\infty}^{\infty} X(\omega)\exp(i\omega t)d\omega, \tag{3.4}$$

$$= \frac{1}{2\pi}\int_{\frac{-\pi}{T}}^{\frac{\pi}{T}} X(\omega)\exp(i\omega t)d\omega,$$

since $X(\omega)$ has no frequency greater than $\frac{\pi}{T}$. Let

$$y(n) = x(nT) = \frac{1}{2\pi}\int_{\frac{-\pi}{T}}^{\frac{\pi}{T}} X(\omega)\exp(i\omega nT)d\omega. \tag{3.5}$$

If we change the variable $\widehat{\omega} = \omega T$,

$$y(n) = \frac{1}{2\pi T}\int_{-\pi}^{\pi} X\left(\frac{\widehat{\omega}}{T}\right)\exp(i\widehat{\omega}n)d\widehat{\omega}. \tag{3.6}$$

On the other hand, from direct Fourier transform,

$$y(n) = \frac{1}{2\pi}\int_{-\pi}^{\pi} Y(\widehat{\omega})\exp(i\widehat{\omega}n)d\widehat{\omega} \tag{3.7}$$

therefore $Y(\widehat{\omega}) = \frac{1}{T}X(\frac{\widehat{\omega}}{T})$ in the range of $-\pi < \widehat{\omega} < \pi$. Thus Y and X have the same shape in this interval even if it is scaled by $\frac{1}{T}$. If Y is known in this range, we can know Y for all frequencies because its period is 2π.

$$Y(\widehat{\omega}) = \frac{1}{T}\sum_{k=-\infty}^{\infty} X\left(\frac{\widehat{\omega} - 2\pi k}{T}\right). \tag{3.8}$$

This relationship is true for any X that is sampled with sampling interval T, regardless of whether a X has frequency components higher than $\frac{\pi}{T}$. Thus if X has higher frequency, there will be overlapping near $-\pi$ and π. This distortion is known as aliasing. It is clearly seen in figure.3.7.

In MRI, aliasing occurs when the sample being imaged extends out of the effective field of view (FOV). The FOV along the x- (frequency encoding gradient G_R) axis is

$$\Delta x = \frac{S_w}{\gamma G_R}, \tag{3.9}$$

where S_w is the signal bandwidth. If we sample the signal at discrete times separated by dwell time (DW), which is just the inverse of the sampling frequency F_s [M.W03], according to Nyquist criterion, $F_s = 2S_w$. Thus the maximum sample size to avoid aliasing is given by

$$\Delta x = \frac{1}{\gamma G_R(2DW)}. \tag{3.10}$$

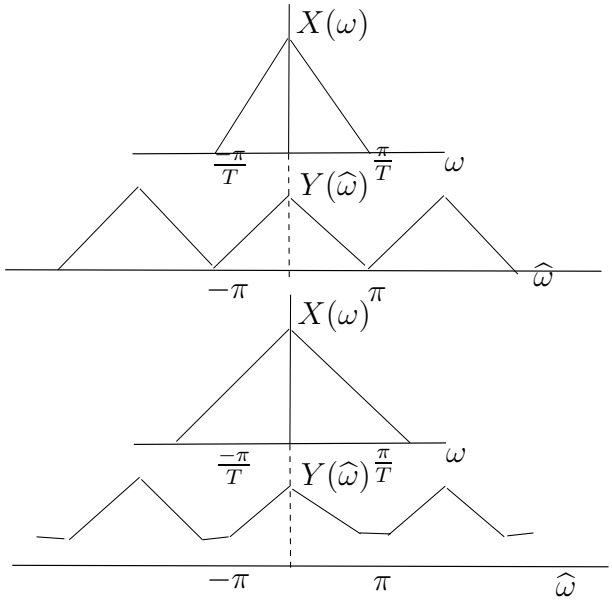

Figure 3.7: Sampling distorts signal if the Nyquist criterion is not fulfilled

The FOV along the y-axis is given by

$$\Delta y = N_p \delta y, \tag{3.11}$$

where $\delta y = \frac{1}{2\gamma G_p t_p}$ is the pixel size and N_p is number of stepping of the phase encoding gradient G_p. The phase encoding gradient is stepped over a range $-G_p$ to $+G_p$ in step of ΔG_p so that $Np = \frac{2G_p}{\Delta G_p}$. Thus

$$\Delta y = \frac{1}{\gamma \Delta G_p t_p}. \tag{3.12}$$

Another artefact occurs when the scanning room is not well shielded from radio waves coming from external sources. The interferance of such wave affects more the signal of high frquency becuase the signal-to-noise ratio is large. When we take the Fourier transform of the signal to decompose into frequency components, there is a frequency overlaping so that it creates a strips in the image perpendicualr to the frequency encoding axis.

4. Summary

The invention of magnetic resonance imaging (MRI) in 1971 by Paul Lauterbur and its subsequent development into a practical, non-invasive means to image tissues inside the body fulfilled a dream long held by physicians. The MRI technique is based on the interactions of nuclear spins in tissues with an external magnetic field. When a system of nuclear spins is exposed to a strong magnetic field $\overrightarrow{B_0}$, more of the spins align themselves along $\overrightarrow{B_0}$ so that the system has a magnetisation $\overrightarrow{M}$. In such a case the spins precess around the field with frequency $\omega_0 = \gamma B_0$. This frequency is known as Larmor frequency. If another magnetic field $\overrightarrow{B_1}$ oscillating with Larmor frequency is applied perpendicular to $\overrightarrow{B_0}$ for a certain time, the magnetisation will be tipped. Then when $\overrightarrow{B_1}$ is turned off, the magnetisation starts to relax and induces an electromagnetic signal. The recovery of the longitudinal magnetisation is characterised by the spin-lattice relaxation time T_1, and the decay of the transversal magnetisation is characterised by spin-spin relaxation time T_2. To reconstruct an image of a given sample we need to calculate the relativite MR signal intensity of slices of the sample. This is possible in MRI, because the Larmor frequency depends on the local magnetic field. Thus by applying a gradient magnetic field, we can select the slice, and we can force the frequencies and the phases to be spatial dependent. These localise the signal. To contrast the signals from different tissues, we can choose T_1,T_2 or proton density of tissues as parameter. In T_1 contrast we use short TR and short TE but to contrast tissues signal due their T_2 difference we use long TR and long TE. In MRI there are many factors that distort the image. These distortions of the image are collectively known as artefacts. Some of the artefacts are caused by parts or whole motion of the sample or the scanner, magnetic susceptibility, aliasing and external RF signals.

Acknowledgement

I would like to express my sincere gratitude to my supervisor Dr. Mark W. Swanepoel for his unreserved support, supervision and friendly approach. I am also indebted to Dr. Sam Webster for his invaluable comments and assisting for the improvement of the essay. I would like to extend my appreciation to Anahita New and Ambrose Chongo for their help by editing the language. Last but not least I would like to thank all AIMS staffs and 2006 AIMS students for their support and friendly spirit that I enjoyed a lot.

This work is dedcated to my lovely mother **Fleku Tebeje**.

Balew Getahun Gelaw

References

[A.P77] A.Papouls, *Signal Analysis, international edition Polytechnic institution of New York*, Mc Graw-Hill Int., 1977.

[Hor] J.P. Hornak, *The basics of MRI, On-line book http://www.cis.rit.edu/htbooks/mri/*.

[Hug91] Michael Hugill, *A comprehensive A-level Course: Advanced Statistics*, Collins Education, 1991.

[MMGP03] Dw McRobbie, EA Moore, MJ Graves, and MR Princes, *MRI: From picture to proton*, Cambridge University Press, 2003.

[M.P] M.Puddephate, *http://www.easymeasure.co.uk/,Principles of Magnetic Resonance Imaging,*.

[M.W03] M.W.Swanepole, *Determination of the diffusion characterstics of ovine intervertebral discs using nuclear magnetic resonance(NMR)*, M.Sc Thesis, Queensland University of Technology, 2003.

[Nay] K.S. Nayak, *Identification and modeling and correction of image artefacts*, http://mre.usc.edu/artifacts, University of Southern California los Angeles California 2005.

[Nol] Douglas Noll, *http://www.eecs.umich.edu/dnoll/bme516/mri1.pdf*, Notes on MRI Part one, 2006.

[Par] C. Leon Partain, *Magnetic resonance imaging-MSN-Encarta*, On-line Encyclopedia 2007.

[Ser90] A.S. Sereway, *Physics for scientists and Engineers third edition*, Saunders Golden Sunbrust series, 1990.

[VBea96] J. Vymazal, M. Babis, and et al., *T1 and T2 alterations in the brains of patients with hepatic cirrhosis*, VYMAZAL. AJNR Am Neuroradio **27** (1996), 333–336.